1 A Plot Twist in Every Day

The file `eopc04.txt` gives daily measurements from the International Earth Rotation and Reference Systems Service (IERS) at the Paris Observatory. It records high-precision daily measurements of Earth's motion and rotation:

- `Date, MJD` — the observation date and the corresponding Modified Julian Date (MJD);
- `x, y` — the position of Earth's North Pole in two orthogonal coordinate directions, in arcseconds;
- `LOD` — Length of Day, the difference, in seconds, between the measured day length and 86 400 seconds. Positive LOD means a longer day.

The Pole's Path

a) Plot the pole's path in the xy-plane. Use the same scale on both axes (an *equal aspect ratio*) so the path keeps its true shape.

b) Find the pole's greatest distance from the origin $(0, 0)$. Give this distance in arcseconds and in meters.

In which year did the pole reach this maximum distance?

The Hidden Period

c) Plot the pole's distance r from the origin against time. Do not smooth the data.

d) The plot shows a complex pattern made by adding two periodic signals. One signal has a period of $T_1 = 365.25$ days. Estimate the second period, T_2.

LOD Trends and Seasonal Changes

e) Convert the LOD values to milliseconds, then plot LOD against time.

f) Fit a straight line $y = kx + b$ to the data, where x is the year and y is LOD in milliseconds. Find the slope k, and express it in milliseconds per century. Compare your result with the known estimate that tidal friction caused by the Moon slows Earth's rotation by about 1.7 milliseconds per century.

g) Subtract the fitted trend from the LOD values in milliseconds to remove the long-term change. Group the residuals by calendar day number (from 1 to 365) and find the average for each day number across all years. Plot the average LOD residual against calendar day number.

h) In which Northern Hemisphere season — winter or summer — are the days longer? Suggest how seasonal changes in Earth's atmosphere might cause this pattern.

Solution

The supplied IERS EOP 14 C04 data contain 23381 daily records from 1962-01-01 to 2026-01-05, with a spacing of one day and no missing dates. The pole coordinates range from $-0.306''$ to $0.324''$ in x and from $-0.023''$ to $0.597''$ in y. The LOD excess ranges from -1.633 to 4.355 ms, so it takes both signs.

The Pole's Path

a) Plot each observed point (x_i, y_i) in chronological order, setting equal scales on the two axes. The trace is the motion of the pole relative to the terrestrial reference-frame origin.

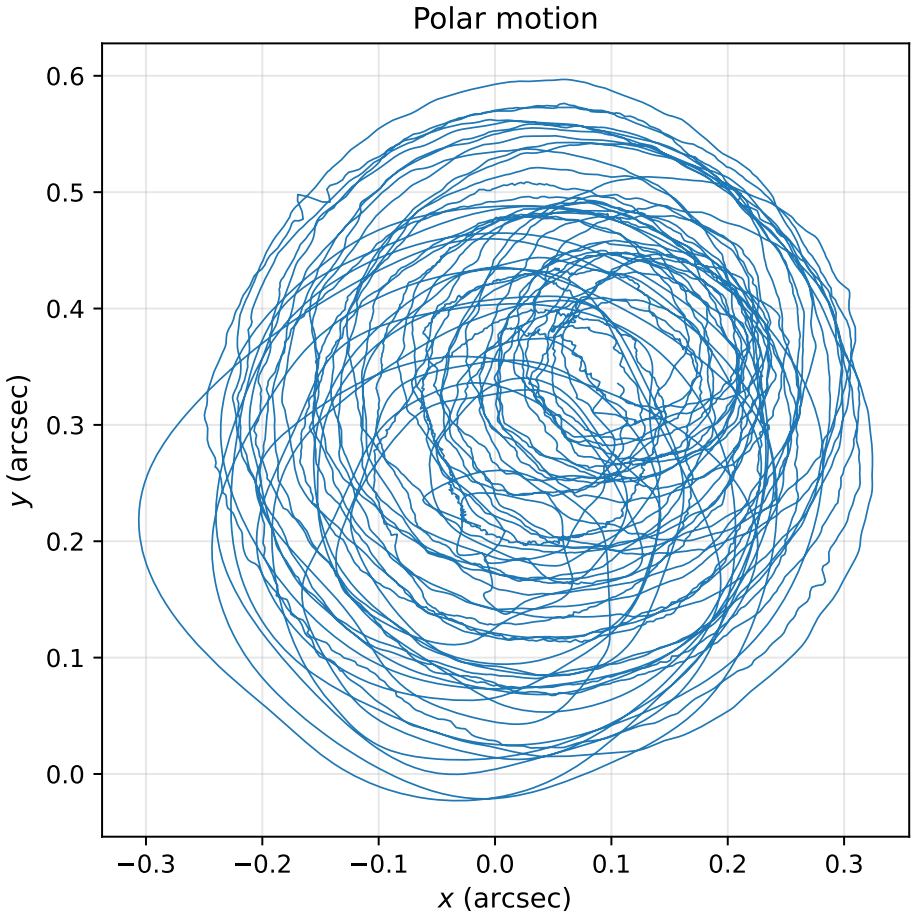

Figure 1: Polar motion in terrestrial xy coordinates

b) For each day compute $r_i = \sqrt{x_i^2 + y_i^2}$. For a small angle r_i in arcseconds, the corresponding surface distance in meters is

$$d_i = R_\oplus \cdot \frac{\pi r_i}{180 \times 3600}, \qquad R_\oplus = 6.371 \times 10^6 \text{ m}.$$

The largest value is $0.600011''$, or 18.53 m, on 1996-06-01 (year 1996).

The Hidden Period

c) Plot the unsmoothed daily values of r_i against decimal year. The envelope grows and shrinks as the annual (T_1) and Chandler (T_2) motions move in and out of phase.

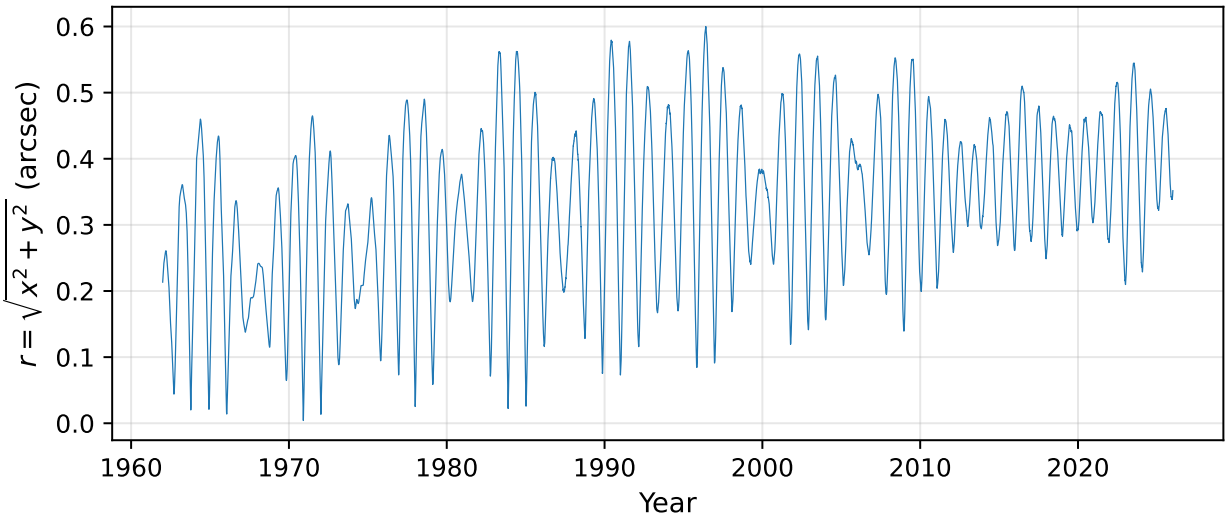

Figure 2: Daily angular distance of the pole from the origin, without smoothing

d) **Synodic-style approach.** Let B be the time between similar peaks of the slow envelope. Reading the plot gives $B \approx 6.4$ yr, or $B \approx 6.4 \times 365.25 \simeq 2340$ d. The two oscillations gain one relative cycle in that time, so

$$\frac{1}{B} = \left|\frac{1}{T_1} - \frac{1}{T_2}\right|, \qquad T_2 = \left(\frac{1}{365.25} - \frac{1}{2340}\right)^{-1} \simeq 433\,\mathrm{d}.$$

Alternative approach: Fitting of two oscillations. The envelope is irregular, so we can refine this estimate using the original x_i and y_i values. For a trial period T, set $u_i = \mathrm{MJD}_i - 49355.0$ and fit each coordinate to

$$a_0 + a_1 u_i + c_1 \sin\frac{2\pi u_i}{365.25} + d_1 \cos\frac{2\pi u_i}{365.25} + c_2 \sin\frac{2\pi u_i}{T} + d_2 \cos\frac{2\pi u_i}{T}.$$

Here, the linear term allows for the observed slow drift. For each T from 400 to 470 d in steps of 0.05 d, determine the six coefficients separately for x and y by linear least squares. Add the squared residuals of both coordinates and choose the T with the smallest sum. This gives $T_2 \simeq 432.60$ d, and hence $B \simeq 6.42$ yr. The fitted coefficients are tabulated.

Coefficient	x	y
a_0 (arcsec)	0.050879	0.301796
a_1 (arcsec/day)	0.000006309	0.000007727
c_1 (arcsec)	−0.085115	0.038647
d_1 (arcsec)	−0.044372	−0.077922
c_2 (arcsec)	0.122008	−0.015596
d_2 (arcsec)	0.014592	0.120739

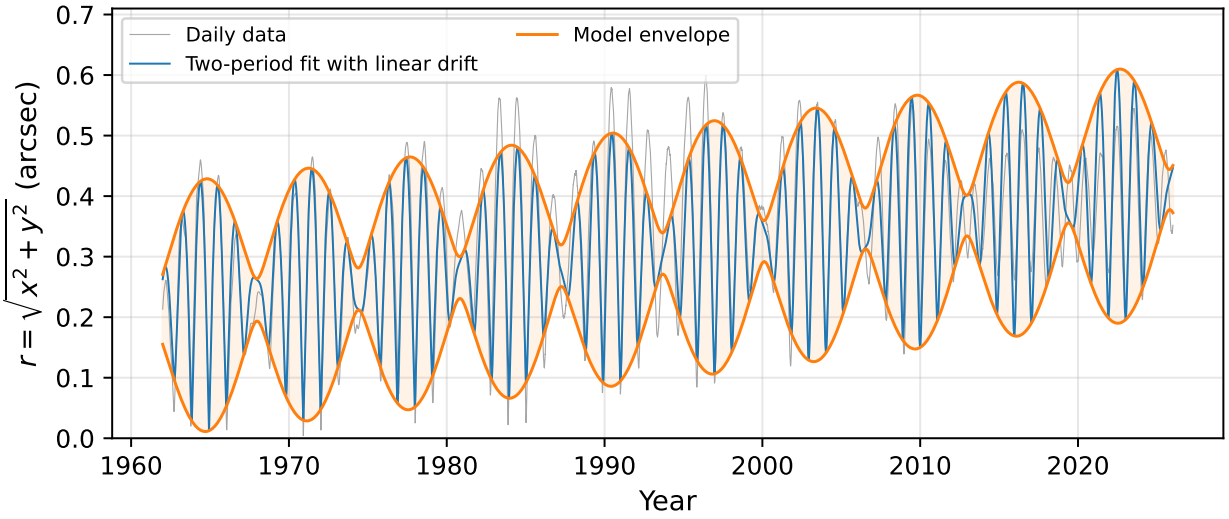

Figure 3: Daily angular distance, the two-period fit with linear drift

The graph above shows $r_{\text{fit}} = \sqrt{x_{\text{fit}}^2 + y_{\text{fit}}^2}$ from this same model. The constant-amplitude model does not reproduce every observed peak, because r also depends on the mean pole offset and changing amplitudes.

LOD Trends and Seasonal Changes

e) Multiply each tabulated LOD value in seconds by 10^3 to obtain milliseconds, then plot it against decimal year.

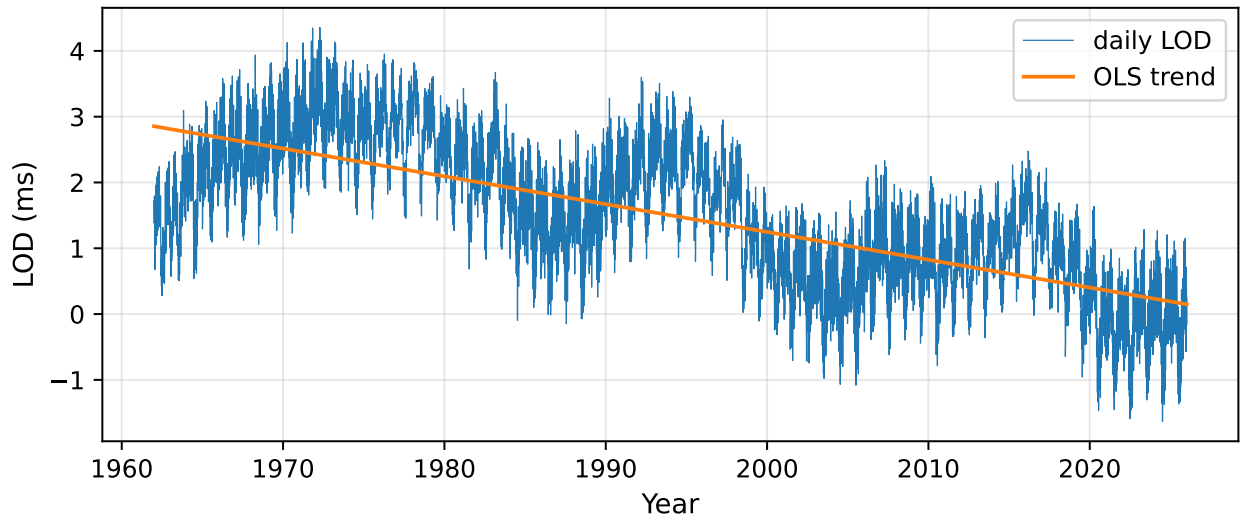

Figure 4: Daily LOD and its least-squares linear trend

f) Fit all daily points $z_i = \mathrm{LOD}_i$ (in ms) with ordinary least squares, using decimal year t_i. The slope is

$$k = \frac{\sum_i (t_i - \bar{t})(z_i - \bar{z})}{\sum_i (t_i - \bar{t})^2} \quad \text{in ms/year}, \qquad k_{\text{century}} = 100k.$$

This gives $k = -0.0422732$ ms/yr $= -4.2273$ ms/century. The observed slope is *negative,* whereas the quoted long-term tidal contribution is +1.7 ms/century. The fitted slope of total LOD over this shorter interval also includes non-tidal changes in Earth's angular momentum, so the two slopes need not agree, even in sign.

g) Set $e_i = z_i - (kt_i + b)$. Omit February 29; for later dates in a leap year subtract one from the ordinal day number. This aligns each calendar date in a common set of days $1, \ldots, 365$. For each day number j, average all available e_i across the years and plot the 365 averages.

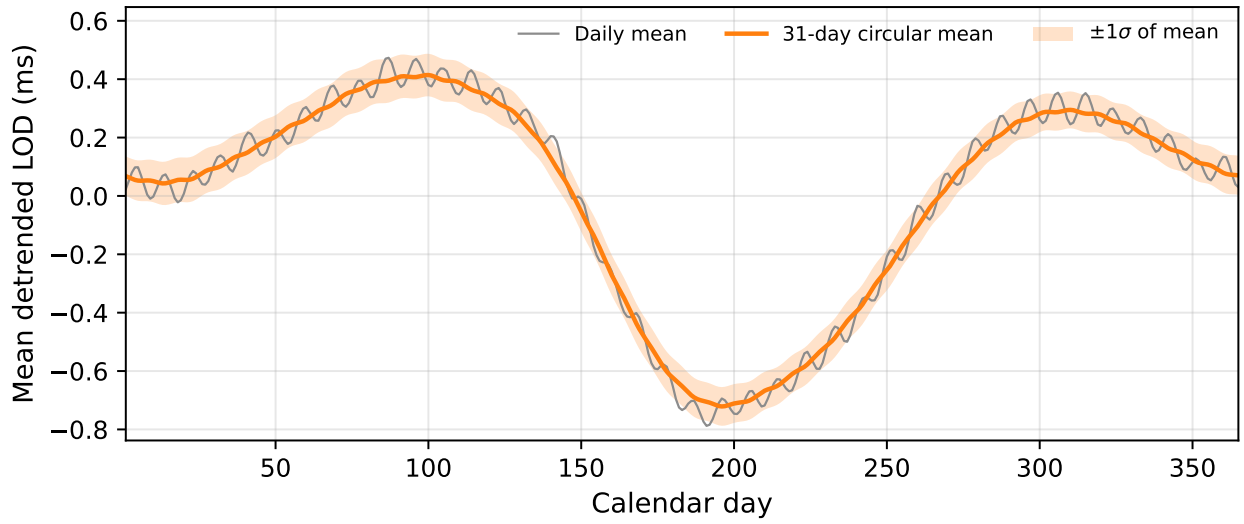

Figure 5: Mean detrended LOD by calendar day.
The orange curve averages the 64 complete annual profiles (1962–2025) after applying a centred 31-day moving average to each, with day numbers wrapped modulo 365. The shaded band is $\pm\sigma_{\text{mean}}$

h) Mean detrended LOD is +0.1153 ms in Northern Hemisphere winter (December–February) and −0.5547 ms in summer (June–August). The difference is 0.6700 ms: winter days are longer.

Stronger winter westerlies carry more eastward atmospheric angular momentum; conservation of angular momentum slows Earth's rotation and raises LOD.

Marking Scheme (25 points):

- **Question (a) The pole's path**
  - **A** Plot of the pole's trajectory in the xy plane with equal scales on both axes **4**
- **Question (b) Maximum pole displacement**
  - **B1** Maximum angular distance, $r_{\max} \simeq 0.600''$ **1**
  - **B2** Conversion to a surface distance, $d_{\max} \simeq 18.5\,\mathrm{m}$ **1**
  - **B3** Year of maximum displacement: 1996 ..... **2**
- **Question (c) Daily angular distance**
  - **C** Plot of the daily angular distance against time without smoothing **4**
- **Question (d) The second period**
  - **D** Estimation of the second period, $T_2 \simeq 433\,\mathrm{d}$ **3**
- **Question (e) Daily LOD excess**
  - **E** Plot of daily LOD excess against time, with LOD in milliseconds **3**
- **Question (f) Long-term trend**
  - **F1** Fitted slope in the required units, $k \simeq -4.23$ ms/century **1**
  - **F2** Comparison with +1.7 ms/century: the fitted trend has the opposite sign and includes non-tidal variations **1**
- **Question (g) Seasonal variation**
  - **G1** Subtraction of the fitted trend and averaging of the residuals across years for each calendar day **1**
  - **G2** Plot of the mean detrended LOD against calendar day number **2**
- **Question (h) Seasonal interpretation**
  - **H1** Correct season: Northern Hemisphere winter **1**
  - **H2** Plausible atmospheric explanation through exchange of angular momentum between the atmosphere and the solid Earth **1**

2 Compact Choir

The file GWs.txt lists mergers of compact objects:

- `Name` — the event name;
- `m1_det` and `m2_det` — the two component masses measured in the detector frame, in $\mathfrak{M}_\odot$;
- `D_L` — the luminosity distance to the event, in megaparsecs (Mpc);
- `z*` — the redshift z.

Assume a flat ΛCDM universe, so $\Omega_\Lambda = 1 - \Omega_m$, and the luminosity distance is

$$D_L(z) = \frac{c(1+z)}{H_0} \int_0^z \frac{d\tilde{z}}{\sqrt{\Omega_m(1+\tilde{z})^3 + \Omega_\Lambda}}.$$

Find the Matter Density

a) The only unknown parameter in the model is Ω_m. Find its best-fit value.

b) Plot the measured luminosity distance D_L against redshift z. Add the theoretical curve using your best-fit value of Ω_m.

Object Masses and Types

A *source-frame mass* is the mass of an object in the rest frame of the binary system. A *detector-frame mass* is the mass inferred from the gravitational-wave signal measured by a detector on Earth, before correcting for redshift. Cosmic expansion redshifts the signal, so the masses are related by

$$m_{\text{det}} = (1+z)m_{\text{src}}.$$

For this task, classify objects with source-frame masses $m \leqslant 2.3\mathfrak{M}_\odot$ as neutron stars (NS), objects with $m \geqslant 3.0\mathfrak{M}_\odot$ as black holes (BH), and objects with $2.3\mathfrak{M}_\odot < m < 3.0\mathfrak{M}_\odot$ as *Uncertain*.

c) For each event, find the total source-frame mass $m_{\text{src}} = m_{1,\text{src}} + m_{2,\text{src}}$. Plot it against redshift z. Describe the main trend. Explain why the plot has this shape.

d) Make a histogram of source-frame component masses. Is there a *mass gap* (a range with few or no objects) between neutron stars and black holes? Justify your answer.

e) Count the following:

- the number of NS, Uncertain, and BH components;
- the number of events with at least one NS;
- the number of events with at least one Uncertain component;
- the number of events in which both objects are BHs.

f) For each event, calculate the mass ratio

$$q = \frac{\min(m_1, m_2)}{\max(m_1, m_2)}.$$

Make a histogram of the q values. What is the median value of q?

g) At merger, the objects emit gravitational waves with a characteristic frequency

$$f_{\text{merger}} \approx \frac{c^3}{G\pi m_{\text{src}}} \cdot \frac{1}{6\sqrt{6}}.$$

Plot frequency against source-frame mass using logarithmic scales on both axes.

What is the frequency range of these events, from the lowest to the highest frequency? Compare it with LIGO's approximate sensitivity range of 10 to 1000 Hz.

Solution

The catalog contains 142 events; note its second header row gives units rather than an event.

Find the Matter Density

a) For each trial Ω_m we calculate

$$D_{L,i}^{\text{model}}(\Omega_m) = \frac{c(1+z_i)}{H_0} \int_0^{z_i} \frac{du}{\sqrt{\Omega_m(1+u)^3 + 1 - \Omega_m}}.$$

We use $H_0 = 67.4\,\text{km}\,\text{s}^{-1}\,\text{Mpc}^{-1}$, which is given in the table of constants.

Since the problem gives no distance uncertainties or fitting rule, our explicit convention is to form the distance residuals $e_i(\Omega_m) = D_{L,i} - D_{L,i}^{\text{model}}(\Omega_m)$ and minimize $S(\Omega_m) = \sum_i e_i(\Omega_m)^2$ over $0 \leqslant \Omega_m \leqslant 1$. The graph shows S against the trial parameter, with the minimum marked.

The best-fit parameter is $\Omega_m = 0.3265$. The measured points lie so close to the model curve that overlaying curves for several trial values also permits *a reasonable estimate by eye,* $\Omega_m \simeq 0.33$.

b) See Figure 7.

Object Masses and Types

c) The total source-frame mass of event i is

$$m_{i,\text{src}} = \frac{m_{1,i,\text{det}} + m_{2,i,\text{det}}}{1 + z_i}.$$

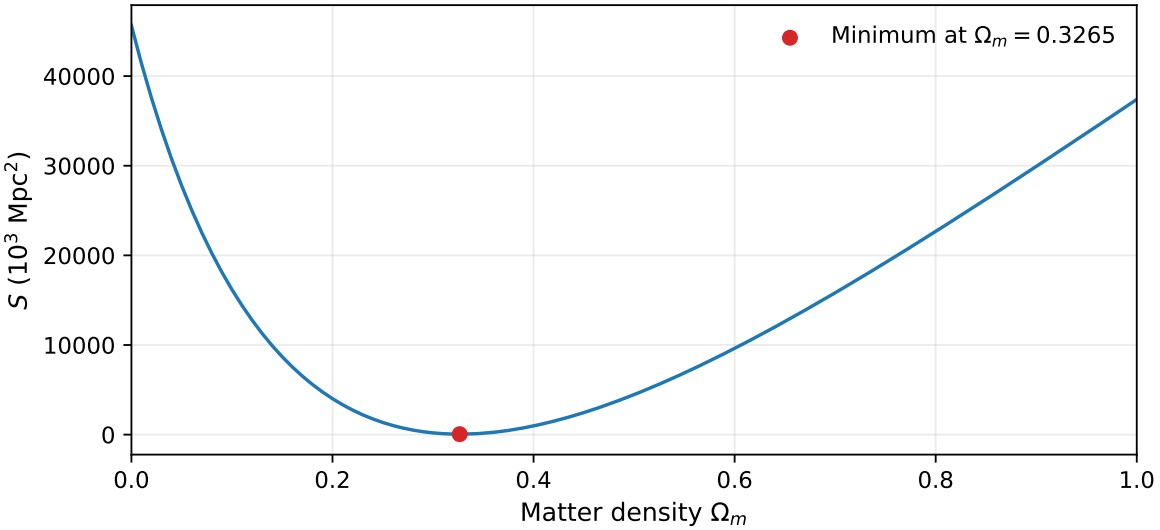

Figure 6: Unweighted sum of squared luminosity-distance residuals versus Ω_m

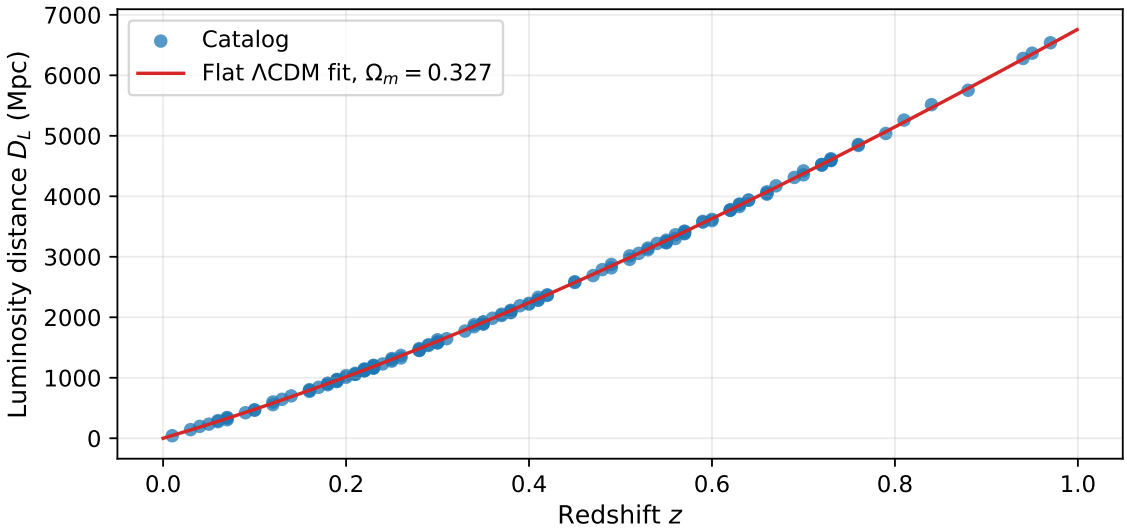

Figure 7: Catalog luminosity distances and the best-fit flat ΛCDM curve

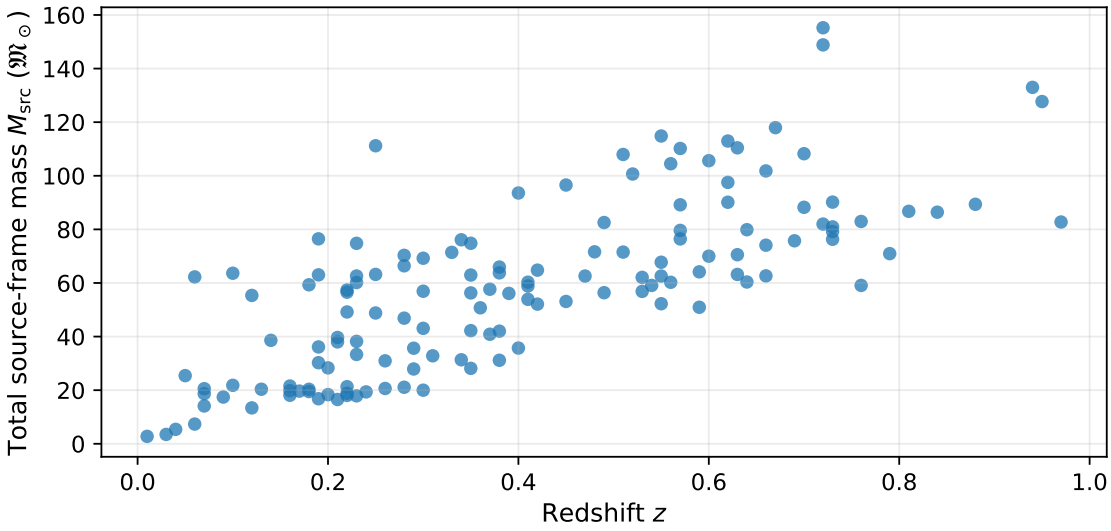

Figure 8: Total source-frame mass of each event versus redshift

The sample shows higher typical source-frame masses at larger redshift: the median is about $20\,\mathfrak{M}_\odot$ for $z \leqslant 0.2$ and $86\,\mathfrak{M}_\odot$ for $0.6 < z \leqslant 1$. *More massive mergers can be detected farther away because their signals are stronger,* which plausibly explains much of this trend; event-to-event mass differences make the scatter. This selection is limited by frequency: $f_{\mathrm{det}} \propto [m_{\mathrm{src}}(1+z)]^{-1}$ here, so sufficiently massive or distant mergers move toward the low-frequency edge of a detector's band.

d) To obtain source-frame masses, we divide each component mass by $1 + z_i$ before making the histogram. See Figures 9 and 10.

The heaviest NS in the catalog is $2.14\,\mathfrak{M}_\odot$, the only Uncertain component is $2.57\,\mathfrak{M}_\odot$, and the lightest BH is $3.85\,\mathfrak{M}_\odot$. There are 2 BHs below $5\,\mathfrak{M}_\odot$. *The interval is sparse but not empty;* mass uncertainties and selection effects limit any claim of a physical gap.

e) We classify each component by its source-frame mass: as an NS if $m_{\mathrm{src}} \leqslant 2.3\,\mathfrak{M}_\odot$, as a BH if $m_{\mathrm{src}} \geqslant 3.0\,\mathfrak{M}_\odot$, and as Uncertain otherwise. We count each event at most once in each requested event category. The counts are

- components: 6 NS, 1 Uncertain, and 277 BH;
- events with at least one NS: 4;
- events with at least one Uncertain component: 1;
- BH–BH events: 137.

f) For every event,

$$q_i = \frac{\min(m_{1,i,\mathrm{src}}, m_{2,i,\mathrm{src}})}{\max(m_{1,i,\mathrm{src}}, m_{2,i,\mathrm{src}})} = \frac{\min(m_{1,i,\mathrm{det}}, m_{2,i,\mathrm{det}})}{\max(m_{1,i,\mathrm{det}}, m_{2,i,\mathrm{det}})},$$

because the common factor $1 + z_i$ cancels. The median is 0.690 (see Figure 11).

g) Inserting m_{src} in solar masses gives

$$f_{\mathrm{merger,src}} \simeq 4.41 \cdot 10^3\,\mathrm{Hz} \times \left(\frac{m_{\mathrm{src}}}{\mathfrak{M}_\odot}\right)^{-1}.$$

A log–log plot is therefore a straight line with slope -1 (see Figure 12).

The sample spans $(28.4 \div 1589.2)$ Hz in the source frame. To compare with LIGO, we must use frequencies in the detector frame:

$$f_{\mathrm{det}} = \frac{f_{\mathrm{src}}}{1+z}, \qquad f_{\mathrm{det}} = (16.5 \div 1573.4)\ \mathrm{Hz}.$$

LIGO's stated $(10 \div 1000)$ Hz band contains 140 of the 142 characteristic detector-frame frequencies; those for GW170817 and GW190425 slightly exceed 1000 Hz (see Figure 13). The formula gives an approximate characteristic frequency, and these two events can still have an inspiral signal within the band.

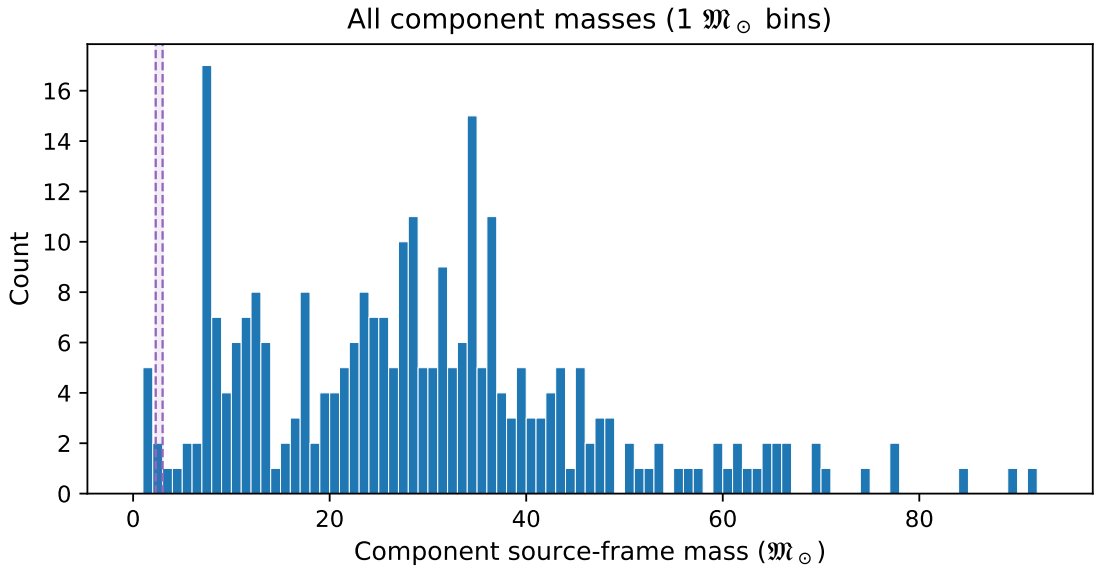

Figure 9: Source-frame component masses for the full catalog

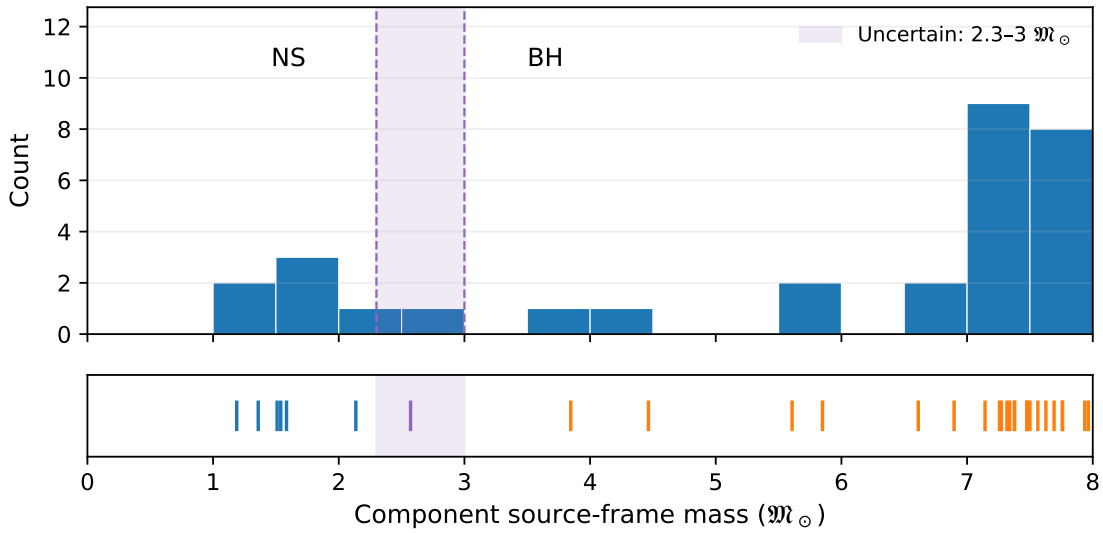

Figure 10: Detailed distribution for small masses

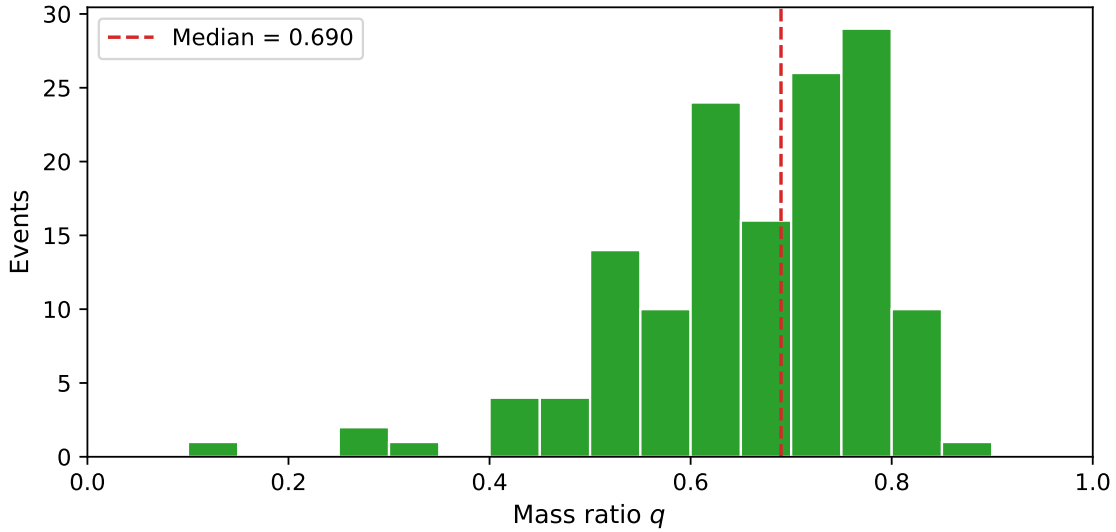

Figure 11: Distribution of component mass ratios q

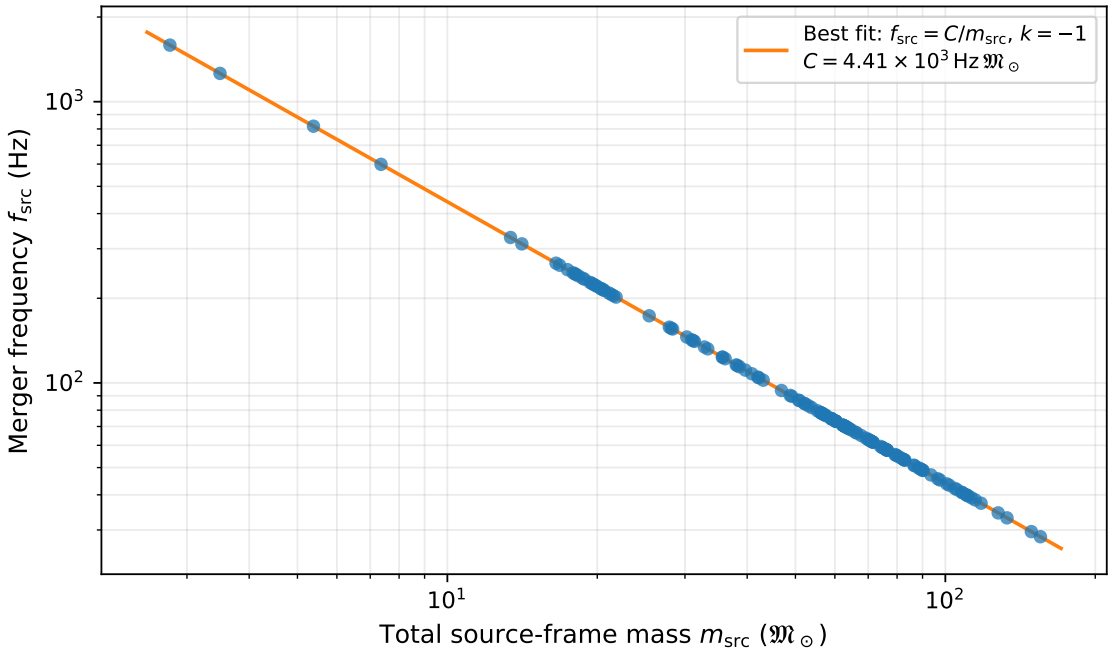

Figure 12: Characteristic **source-frame** merger frequency against total source-frame mass

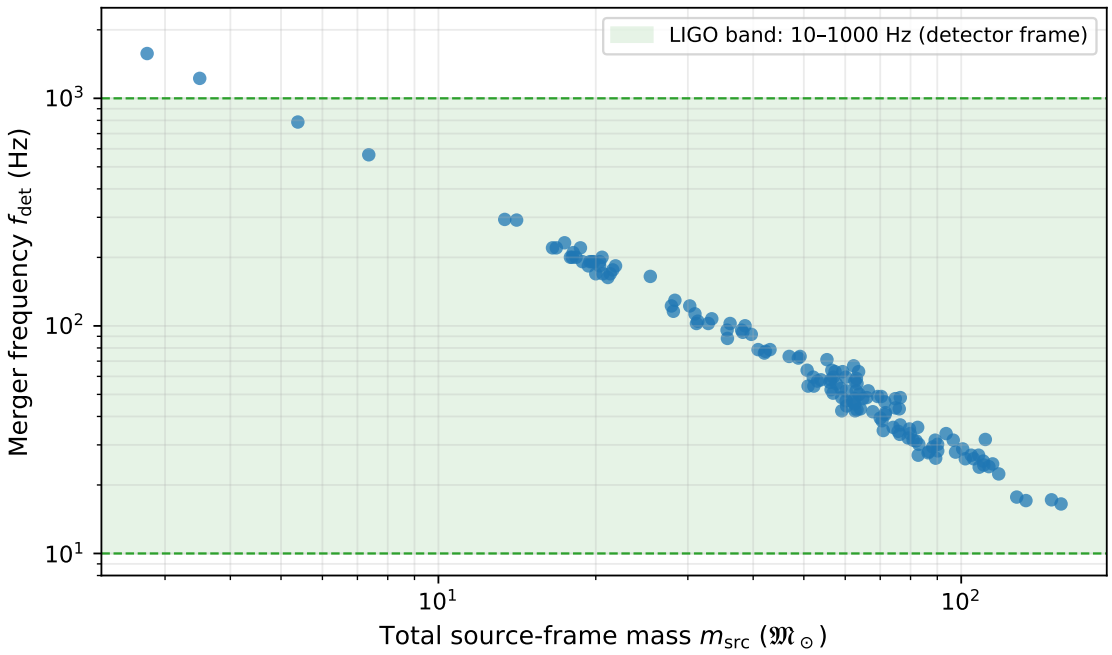

Figure 13: Characteristic **detector-frame** merger frequency against total source-frame mass

Marking Scheme (25 points):

- **Question (a) Matter density**
  - **A1** Valid method for fitting model luminosity distances to the data **2**
  - **A2** Correct matter-density estimate, $\Omega_m \simeq 0.33$ **2**
- **Question (b) Distance–redshift relation**
  - **B1** Plot of the catalog luminosity distances against redshift **3**
  - **B2** Theoretical curve for the adopted best-fit Ω_m on the same plot **1**
- **Question (c) Source-frame masses**
  - **C1** Plot of total source-frame mass against redshift **2**
  - **C2** Description and explanation of the trend: typical observed masses increase with redshift, mainly because more massive mergers are detectable farther away **2**
- **Question (d) Component masses and the mass gap**
  - **D1** Histogram of source-frame component masses for the full catalog **1**
  - **D2** Enlarged low-mass histogram resolving the NS–BH transition and supporting the mass-gap assessment **2**
- **Question (e) Object and event counts**
  - Component counts: 6 NS, 1 Uncertain, and 277 BH **1**
  - Events with at least one NS: 4 ..... **1**
  - Events with at least one Uncertain component: 1 ..... **1**
  - BH–BH events: 137 ..... **1**
  - **E Subtotal 4**
- **Question (f) Mass ratios**
  - **F1** Histogram of the component mass ratios q **2**
  - **F2** Median mass ratio, $q_{\mathrm{med}} \simeq 0.690$ **1**
- **Question (g) Merger frequencies**
  - **G1** Log–log plot of merger frequency against total source-frame mass **2**
  - **G2** Frequency range: $(28.4 \div 1589)$ Hz in the source frame; $(16.5 \div 1573)$ Hz in the detector frame for comparison with LIGO **1**

3 A Comet's Visit

On 17 January 2016, comet C/2013 US10 (Catalina) was close to its nearest point to Earth. Its horizontal parallax was $\approx 12''$. On 18 March 2016, the horizontal parallax was $\approx 4.0''$.

A simple estimate

a) Use the horizontal parallax values to find the distance from Earth to the comet on 17 January and on 18 March. Give your answers in astronomical units.

b) Assume that the comet moved in a *straight line* relative to Earth. Take 17 January as the moment of closest approach. Estimate the relative distance it travelled in 61 days and its average relative speed in km/s.

Keplerian motion

The table below gives approximate starting positions and velocities on 17 January 2016 at 06:00 UTC. The Sun is at the origin, the coordinate axes are fixed, and the xy plane is the ecliptic plane.

	Earth	**Comet**
x (AU)	-0.43622849	-0.80691474
y (AU)	$+0.88172514$	$+0.94496430$
z (AU)	-0.00003220	$+0.61939535$
v_x (AU/day)	-0.01570046	$+0.00524790$
v_y (AU/day)	-0.00769377	$+0.01726800$
v_z (AU/day)	$+0.00000028$	$+0.01002658$

c) Calculate the positions of Earth and the comet for the next 61 days considering Keplerian motion.

d) For each day, find the comet's position relative to Earth. Plot the comet's relative path in the ecliptic plane.

e) Find the total length of the comet's path relative to Earth during these 61 days. Calculate its average relative speed in km/s.

How curved was the relative path?

f) Compare the average path speed from part (e) with the simple estimate from part (b). Find the percentage difference.

g) Make a second model in which the comet moves relative to Earth in a straight line, keeping its initial relative velocity. On the same graphs, plot the actual (Keplerian-model) relative path and the straight-line path in the xy and xz planes.

h) Find the distance between the two predicted positions of the comet after 61 days in AU.

i) Based on your results, which quantity is better estimated by the second straight-line model defined in part (g): the average relative speed or the comet's relative position after 61 days? Justify your answer.

Solution

We use $R_\oplus = 6371\,\text{km}$, $1\,\text{au} = 1.496 \times 10^8\,\text{km}$, and $1\,\text{day} = 86400\,\text{s}$ from the constants table. All Cartesian heliocentric vectors below use the Sun as origin and the non-rotating axes of the initial-state table, with the xy plane in the ecliptic. Relative vectors use the same axis directions but have their origin at Earth's instantaneous position.

a) Horizontal parallax p is the angle subtended by Earth's radius at the comet:

$$d = \frac{R_\oplus}{\sin p}.$$

The two distances are

$$d_{17\,\text{Jan}} = 0.7320\,\text{au},$$
$$d_{18\,\text{Mar}} = 2.1960\,\text{au}.$$

b) At closest approach, the straight-line direction of motion is perpendicular to the Earth–comet radius. The distances therefore form a right triangle. Put Earth at the origin of a local diagram, with one axis along the comet's straight path:

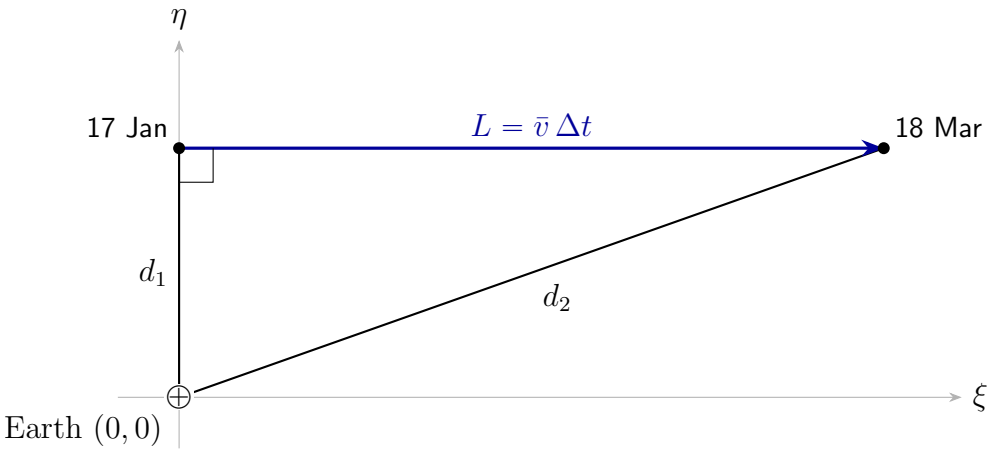

Figure 14: Straight-line closest-approach geometry, with Earth at the origin

$$L_{\text{simple}} = \sqrt{d_{18\,\text{Mar}}^2 - d_{17\,\text{Jan}}^2} = 2.0705\,\text{au}.$$

$$\bar{v}_{\text{simple}} = \frac{L}{\Delta t} = 58.77\,\text{km}\,\text{s}^{-1} \approx 59\,\text{km}\,\text{s}^{-1}.$$

c) Integrate the motion of Earth and the comet separately in the Sun's gravitational field, starting from the position and velocity vectors in the table.

For either body,

$$\frac{d\boldsymbol{r}}{dt} = \boldsymbol{v},$$
$$\frac{d\boldsymbol{v}}{dt} = \boldsymbol{a}(\boldsymbol{r}) = -\frac{G\mathfrak{M}_\odot}{|\boldsymbol{r}|^3}\boldsymbol{r}.$$

The simplest choice is the *forward Euler scheme*. At each step, calculate $\boldsymbol{a}_n = \boldsymbol{a}(\boldsymbol{r}_n)$ and set

$$\boldsymbol{r}_{n+1} = \boldsymbol{r}_n + h\boldsymbol{v}_n,$$
$$\boldsymbol{v}_{n+1} = \boldsymbol{v}_n + h\boldsymbol{a}_n.$$

Both updates use the old position and velocity. Repeat for each body up to $t = 61\,\mathrm{d}$, saving the positions at $t = 0, 1, \ldots, 61\,\mathrm{d}$.

The *velocity-Verlet scheme* gives better accuracy for the same step:

$$\boldsymbol{r}_{n+1} = \boldsymbol{r}_n + h\boldsymbol{v}_n + \frac{1}{2}h^2\boldsymbol{a}_n,$$
$$\boldsymbol{v}_{n+1} = \boldsymbol{v}_n + \frac{1}{2}h\big(\boldsymbol{a}_n + \boldsymbol{a}_{n+1}\big),$$

where $\boldsymbol{a}_{n+1}$ is calculated at the new position. A standard adaptive *Runge–Kutta solver* is also suitable. For the reference calculation below, we use an eighth-order method with relative tolerance 10^{-11}, absolute tolerance 10^{-13}, and maximum step $0.25\,\mathrm{d}$.

All three methods give the same rounded answers, and halving the fixed steps does not change them. *Any* sufficiently accurate method is acceptable.

Another valid approach uses the analytic Keplerian solution in terms of orbital anomalies: find each orbit's plane and orientation from the initial vectors, solve Kepler's equation at each date, and rotate the position back to the given axes. This follows the exact two-body orbit but involves more geometry.

The reference calculation gives the following positions at day 61:

$$\boldsymbol{r}_\oplus = (-0.994626,\ +0.037282,\ -0.000001)\,\mathrm{au},$$
$$\boldsymbol{r}_\mathrm{C} = (-0.394636,\ +1.842613,\ +1.131597)\,\mathrm{au}.$$

d) Subtract Earth's position from the comet's at each time: $\boldsymbol{\rho}(t) = \boldsymbol{r}_{\mathrm{C}}(t) - \boldsymbol{r}_{\oplus}(t)$. The xy projection and some values of (ρ_x, ρ_y, ρ_z) are shown below.

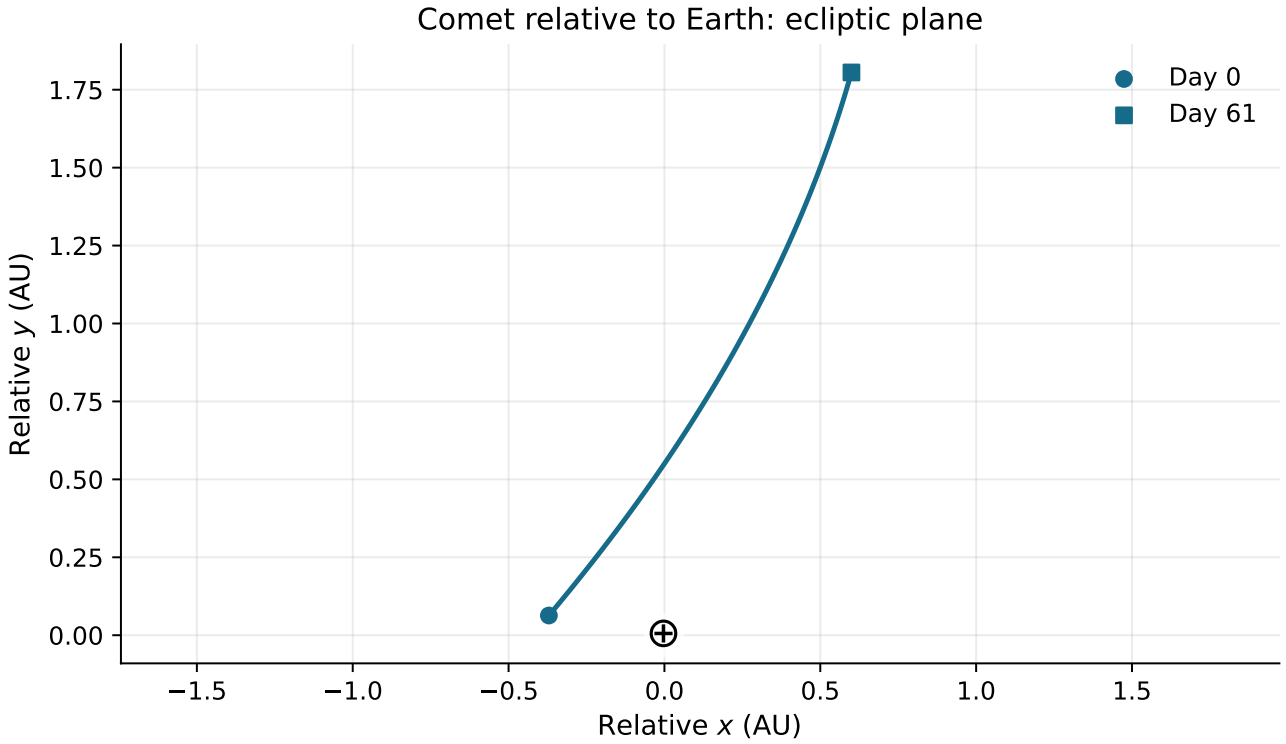

Figure 15: Comet position relative to Earth projected onto the ecliptic (xy) plane

e) Add the lengths of the 61 straight segments between consecutive daily relative positions $\boldsymbol{\rho}_j = \boldsymbol{\rho}(j\,\mathrm{d})$. Use all three coordinates, including z:

$$L_{\mathrm{Kep}} \simeq \sum_{j=0}^{60} \left|\boldsymbol{\rho}_{j+1} - \boldsymbol{\rho}_j\right| = 2.074150\,\mathrm{au},$$

$$\bar{v}_{\mathrm{Kep}} = \frac{L_{\mathrm{Kep}}}{\Delta t} \simeq 58.875\,\mathrm{km\,s^{-1}}.$$

day	ρ_x, au	ρ_y, au	ρ_z, au
0	−0.370686	0.063239	0.619428
15	−0.065841	0.455805	0.762584
30	0.206011	0.879522	0.893024
45	0.428500	1.323867	1.013039
61	0.599991	1.805331	1.131598

Using a finer grid with 0.01 d intervals gives $L_{\mathrm{Kep}} = 2.074154\,\mathrm{au}$, a change of only about $4 \cdot 10^{-6}\,\mathrm{au}$. The daily positions are already sufficient for this estimate.

f) Relative to the simple estimate in (b), the average-speed difference is

$$\frac{|58.875 - 58.770|}{58.770} \times 100\,\% = 0.18\,\%.$$

g) The straight-line model keeps the initial relative velocity:

$$\boldsymbol{\rho}_{\mathrm{line}}(t) = \boldsymbol{\rho}(0) + \big[\boldsymbol{v}_{\mathrm{C}}(0) - \boldsymbol{v}_{\oplus}(0)\big]t.$$

Both projected paths are plotted together in each requested plane below.

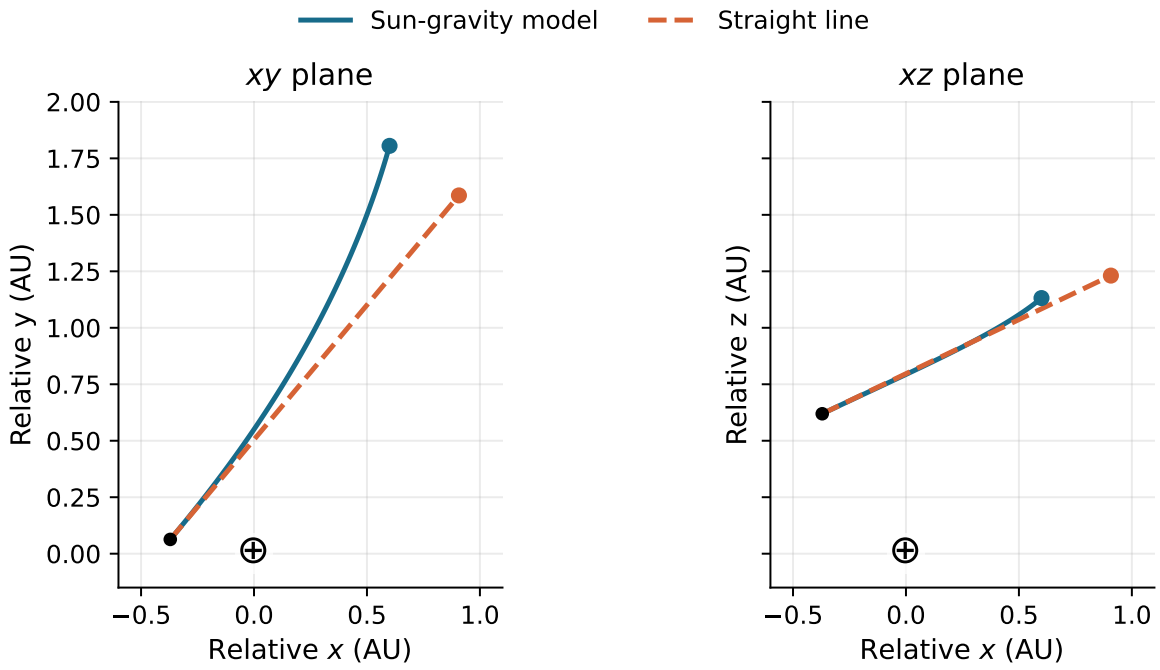

Figure 16: Keplerian and constant-velocity relative paths in the xy and xz planes

h) At day 61, the Keplerian and straight-line relative positions are respectively $(0.599991,\ 1.805331,\ 1.131598)$ au and $(0.907164,\ 1.585907,\ 1.231032)$ au.
Their three-dimensional separation is 0.39037 au.

i) The second straight-line model in (g) estimates the average relative speed much better than the final relative position:

- *Average relative speed.* The line has constant speed

$$\bar{v}_{\text{line}} = |\boldsymbol{v}_{\text{C}}(0) - \boldsymbol{v}_{\oplus}(0)| \simeq 0.0340947\,\frac{\text{au}}{\text{day}} \times \frac{1.496 \times 10^8\,\text{km/au}}{86400\,\text{s/day}} \simeq 59.034\,\text{km}\,\text{s}^{-1}.$$

  Relative to $\bar{v}_{\text{Kep}} = 58.875\,\text{km}\,\text{s}^{-1}$, its error is

$$\epsilon_v = \frac{|59.034 - 58.875|}{58.875} \times 100\,\% \simeq 0.27\,\%.$$

- *Relative position after 61 days.* With $\Delta\rho = 0.39037$ au from (h),

$$\left|\boldsymbol{\rho}_{\text{Kep}}(61)\right| = \sqrt{0.599991^2 + 1.805331^2 + 1.131598^2} = 2.21353\,\text{au},$$
$$\epsilon_r = \frac{0.39037}{2.21353} \times 100\,\% \simeq 17.6\,\%.$$

The fractional position error is about 65 times the fractional speed error. Solar gravity bends the relative path, so similar average path speeds do not imply similar endpoint positions.

Marking Scheme (25 points):

- **Question (a) Distances from parallax**

  A Earth–comet distances: 0.73 au on 17 January and 2.20 au on 18 March **2**
  1 point for each correctly calculated distance.

- **Question (b) Straight-line estimate**

  B Right-triangle geometry and the resulting path length $L \simeq 2.07\,\mathrm{au}$ and average speed $\bar{v} \approx 59\,\mathrm{km\,s^{-1}}$ **4**
  2 points for the geometry and 2 points for the numerical result.

- **Question (c) Keplerian positions**

  C Calculation of both bodies' daily heliocentric positions by a valid method **4**
  2 points for the method and 2 points for the results.

- **Question (d) Relative trajectory**

  D Plot of the comet's Earth-relative path in the ecliptic plane **2**

- **Question (e) Path length and average speed**

  E Three-dimensional relative path length $L \simeq 2.074\,\mathrm{au}$ and average relative speed $\bar{v} \simeq 58.9\,\mathrm{km\,s^{-1}}$ **4**
  2 points for the path length and 2 points for the average speed.

- **Question (f) Comparison with the simple estimate**

  F Percentage difference between the speeds in (b) and (e), about 0.2 % **2**

- **Question (g) Comparison of projected paths**

  G Keplerian and straight-line paths plotted together in the xy and xz planes **2**
  1 point for the xy plot and 1 point for the xz plot.

- **Question (h) Final position difference**

  H Separation of the predicted positions after 61 days, $\Delta\rho \simeq 0.4\,\mathrm{au}$ **2**

- **Question (i) Accuracy of the second straight-line model**

  I Justified conclusion that the average speed is better estimated **3**
  1 point for the conclusion and 2 points for the justification.

Constants

Universal

Gravitational constant	$G = 6.67 \cdot 10^{-11}\ \frac{\mathrm{m}^3}{\mathrm{kg \cdot s}^2}$
Speed of light	$c = 3.00 \cdot 10^8$ m/s

Astronomical

Astronomical unit	$1\ \mathrm{au} = 149.6 \cdot 10^6$ km
Parsec	$1\ \mathrm{pc} = 206\,265\ \mathrm{au}$
Hubble constant	$H_0 = 67.4$ (km/s)/Mpc

Emission constants

Stefan–Boltzmann	$\sigma = 5.67 \cdot 10^{-8}\ \frac{\mathrm{W}}{\mathrm{m}^2 \cdot \mathrm{K}^4}$
Wien's displacement	$b = 2898\ \mu\mathrm{m} \cdot \mathrm{K}$

Earth

Radius	$R_\oplus = 6371$ km
Obliquity of ecliptic	$\varepsilon = 23.4^\circ$
Orbital period	$T_\oplus = 365.26$ days

Sun

Radius	$R_\odot = 6.96 \cdot 10^5$ km
Mass	$\mathfrak{M}_\odot = 1.99 \cdot 10^{30}$ kg
Absolute magnitude	$M_\odot = 4.74^{\mathrm{m}}$ (bol.)
Effective temperature	$T_\odot = 5.8 \cdot 10^3$ K
Luminosity	$L_\odot = 3.828 \cdot 10^{26}$ W